Journal of Sound and Vibration (2002) 254(3), 541–555
doi:10.1006/jsvi.2001.4109, available online at http://www.idealibrary.com on IDEAL®

THE DYNAMIC STIFFNESS MATRIX METHOD IN FORCED VIBRATION ANALYSIS OF MULTIPLE-CRACKED BEAM

N. T. KHIEM

Institute of Mechanics, National Centre for Natural Science Technology of Vietnam, Vien co Hoc, 264, Doi Can, Hanoi, Vietnam. E-mail: ntkhiem@im01.ac.vn

AND

T. V. LIEN

Hanoi University of Civil Engineering, 55, Giai Phong Road, Hanoi, Vietnam

(*Received* 14 *June* 2001, *and in final form* 12 *October* 2001)

The dynamic behaviour of a beam with numerous transverse cracks is studied. Based on the equivalent rotational spring model of crack and the transfer matrix for beam, the dynamic stiffness matrix method has been developed for spectral analysis of forced vibration of a multiple cracked beam. As a particular case, when the excitation frequency is close to zero, the solution for static response of beam with an arbitrary number of cracks has been obtained exactly in an analytical form. In general case, the effect of crack number and depth on the dynamic response of beam was analyzed numerically.

1. INTRODUCTION

The vibration analysis of cracked beams or shafts is a problem of great interest due to its practical importance. The change in dynamical characteristics such as one-dimensional structure due to cracks is most useful in crack location and depth evaluation. Because of this, many works devoted to the free vibration analysis of cracked beams of shafts were published [1–11]. Based on the studies, some procedures for crack detection are developed in the case of single- or double-cracked beam. On the other hand, there are fewer studies on the dynamic response of cracked beam to external excitation [12, 13]. In the previous studies, the beam with only single crack had been investigated. The dynamic response of cracked beam to external load may be used in the modal testing, crack identification, as well as in the reanalysis of structures after damage detection. In this paper, the forced vibration of a multiple-cracked beam is considered using the dynamic stiffness matrix method developed herein.

In general, transverse crack causes change in the cross-section and consequently, introduces a local flexibility to the beam. To study the effect of crack on the vibration of a beam, both the analytical and finite element methods are applied. An analytical method such as the transfer matrix method (TMM), for example, in conjugation with a suitable model of crack, allows to study vibration of cracked beam with respect to geometry (depth and location) of crack [4–8]. However, this approach is difficult to be used in structures other than beams such as, for example, a frame. A combination of the finite element methods (FEM) and the TMM has been developed in reference [1] for vibration analysis of

0022-460X/02/$35.00

beam with abrupt changes of cross-section. A specification of the FEM application to vibration analysis of cracked beam has been proposed in reference [12]. The use of the FEM in analysis of more complex structures with cracked members in general, requires to "smooth" the local flexibility of crack as a change in stiffness or elasticity modulus [3] of a beam element containing the crack. To overcome this the authors of reference [13] have conjugated the FEM with the idea of a compliance matrix to develop a specific technique for vibration analysis of cracked beam. This development made the FEM suitable for analysis of frame structures with the local flexibility due to a crack in its members [14, 15]. The results of such developed FEM application to a cracked beam are still approximate in comparison with the analytical methods. The idea is to extend the advantages of the analytical method to more complex structures other than beams so as to develop in this paper the dynamic stiffness matrix method for a cracked beam element. The dynamic stiffness matrix (DSM) method developed for cracked beam overcomes the above-mentioned limitations of the analytical and FEMs. In fact, the DSM method as an exact one [16–18] holds the advantage of the analytical method in consideration of crack as local change of cross-section. Simultaneously, the DSM method can be applied to more complex structures other than beams due likely to the FEM formulation. In addition, it is necessary to note that the DSM method leads to the FEM as it is only an approximation.

Based on the concept of the equivalent spring model of crack substantiated basically in reference [5], the goal of this paper is to develop the DSM method for vibration analysis of a multiple-cracked beam. To illustrate the theory developed here, the response of a beam with an arbitrary number of cracks to external load is investigated using the DSM method. First, the static response has been obtained analytically as a particular case by letting the excitation frequency be close to zero. The obtained formulas in the static case for displacements are useful for crack detection by static test. The response to a dynamic load in the frequency domain can be investigated only numerically. In this case, the displacement, slope, bending moment and shear force are computed depending on the number and depth of cracks. Comparing the results obtained in the present paper with those given in references [12, 13] leads to some comments on the efficiency of the proposed method.

2. VIBRATION MODEL OF BEAM WITH n CRACKS

A beam of length L, cross-section area $A = b \times h$, second moment of the area I and Young's modulus E is considered. Suppose that the beam has been cracked at a number of positions $x_1, \ldots, x_n$, which are positive and ordered in an increasing sequence. Furthermore, introducing $x_0 = 0$; $x_{n+1} = L$, one gets a set of positions $\{x_j, j = 0,1,2, \ldots, n, n+1\}$. The cracks at x_j are modelled, as shown in Figure 1, by rotational spring of stiffness [5]

$$K_j = \frac{1}{\alpha_j}, \quad \alpha_j = \frac{6\pi(1 - v^2)h}{EI} I_c\left(\frac{a_j}{h}\right), \tag{1}$$

where v is the Poisson coefficient, h the beam height, and a_j is the crack depth. The function $I_c(z)$ as shown in reference [5] can be taken, for example, in the form

$$I_c(z) = 0{\cdot}6272z^2 - 1{\cdot}04533z^3 + 4{\cdot}5948z^4 - 9{\cdot}973z^5 + 20{\cdot}2948z^6$$
$$- 33{\cdot}0351z^7 + 47{\cdot}1063z^8 - 40{\cdot}7556z^9 + 19{\cdot}6z^{10}.$$

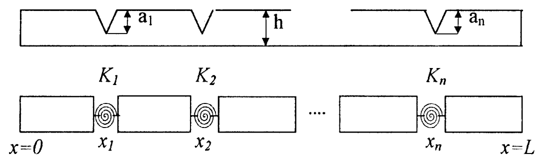

Figure 1. Modelling of multiple-cracked beam.

Vibration of the beam is described by the equation

$$EI\left[\frac{\partial^4 w(x,t)}{\partial x^4}+\mu_1\frac{\partial^5 w(x,t)}{\partial x^4\partial t}\right]+\rho A\left[\frac{\partial^2 w}{\partial t^2}+\mu_2\frac{\partial w}{\partial t}\right]=q(x,t), \tag{2}$$

where $w=w(x,\ t)$ is the transverse displacement of the beam at the section x, μ_1, μ_2 are the material and viscous damping coefficients, $q(x,t)$ the distributed load. Using the Fourier representation for the vibration and the load

$$w(x,t)=\Phi(x,\omega)\mathrm{e}^{-\mathrm{i}\omega t},\qquad q(x,t)=\hat{q}(x,\omega)\mathrm{e}^{-\mathrm{i}\omega t}, \tag{3}$$

where $\Phi(x,\omega)$; $\hat{q}(x,\omega)$ denote complex amplitude of the vibration and load, respectively, one gets the equation

$$\frac{\mathrm{d}^4\Phi(x,\omega)}{\mathrm{d}x^4}-\lambda^4\Phi(x,\omega)=\bar{q}(x,\omega), \tag{4}$$

where

$$\lambda^4=\omega^2\frac{\rho A(1-\mathrm{i}\mu_2/\omega)}{EI(1+\mathrm{i}\mu_1\omega)},\qquad \tilde{q}(x,\omega)=\frac{\hat{q}(x,\omega)}{EI(1+\mathrm{i}\mu_1\omega)}.$$

Equation (4) must be investigated with the conditions at the crack position x_j:

$$\Phi(x_j-0)=\Phi(x_j+0),\quad \Phi''(x_j-0)=\Phi''(x_j+0),\quad \Phi'''(x_j-0)=\Phi'''(x_j+0),$$

$$\Phi'(x_j-0)+\beta_j\Phi''(x_j-0)=\Phi'(x_j+0),\quad \beta_j=EI\,\alpha_j=\frac{EI}{k_j}=6\pi(1-v^2)hI_c\left(\frac{a_j}{h}\right) \tag{5}$$

and the boundary conditions, which can be expressed in the form

$$\underline{B}_1^0\begin{pmatrix}\Phi(+0)\\ \Phi'(+0)\end{pmatrix}+\underline{B}_2^0\begin{pmatrix}EI\,\Phi'''(+0)\\ -EI\,\Phi''(+0)\end{pmatrix}=0,$$

$$\underline{B}_1^L\begin{pmatrix}\Phi(L-0)\\ \Phi'(L-0)\end{pmatrix}+\underline{B}_2^L\begin{pmatrix}-EI\,\Phi'''(L-0)\\ EI\,\Phi''(L-0)\end{pmatrix}=0 \tag{6}$$

with the 2×2 dimension matrices

$$\underline{\mathbf{B}}_1^0=\begin{pmatrix}B_{11}^0 & B_{12}^0\\ B_{21}^0 & B_{22}^0\end{pmatrix},\quad \underline{\mathbf{B}}_2^0=\begin{pmatrix}B_{13}^0 & B_{14}^0\\ B_{23}^0 & B_{24}^0\end{pmatrix},$$

$$\underline{\mathbf{B}}_1^L=\begin{pmatrix}B_{11}^L & B_{12}^L\\ B_{21}^L & B_{22}^L\end{pmatrix},\quad \underline{\mathbf{B}}_1^L=\begin{pmatrix}B_{13}^L & B_{14}^L\\ B_{23}^L & B_{24}^L\end{pmatrix},$$

where B_{ij}^0, B_{ij}^L are boundary parameters.

3. THE DYNAMIC STIFFNESS MATRIX METHOD

In this section, the following notations are introduced:

$$\bar{\mathbf{Z}}^-(j) = \{Z_1^-(j), Z_2^-(j), Z_3^-(j), Z_4^-(j)\}^{\mathrm{T}},$$

$$\bar{\mathbf{Z}}^+(j) = \{Z_1^+(j), Z_2^+(j), Z_3^+(j), Z_4^+(j)\}^{\mathrm{T}}, \quad j = 0, 1, 2, \dots, n+1,$$

$$Z_1^\pm(j) = \Phi(x_j \pm 0), \quad Z_2^\pm(j) = \Phi'(x_j \pm 0),$$

$$Z_3^\pm(j) = \pm EI\Phi'''(x_j \pm 0), \quad Z_4^\pm(j) = \mp EI\Phi''(x_j \pm 0),$$

$$Z_1^+(0) = \Phi(0) = U_1, \quad Z_2^+(0) = \Phi'(0) = U_2,$$

$$Z_3^+(0) = EI\Phi''(0) = P_1, \quad Z_4^+(0) = -EI\Phi''(0) = P_2,$$

$$Z_1^-(n+1) = \Phi(L) = U_3, \quad Z_2^-(n+1) = \Phi'(L) = U_4,$$

$$Z_3^-(n+1) = -EI\Phi'''(L) = P_3,$$

$$Z_4^-(n+1) = EI\Phi''(L) = P_4.$$

Then general solution of equation (4) for $x \in (x_{j-1}, x_j)$, $j = 1, 2, \dots, n+1$, has the form

$$\Phi(x) = \Phi_0(\bar{x}) + \frac{1}{\lambda^3}\int_0^{\bar{x}} K_4(\lambda(\bar{x}-\tau))\tilde{q}(x_{j-1}+\tau, \omega)\,\mathrm{d}\tau, \quad x \in [x_{j-1}, x_j], \quad \bar{x} = x - x_{j-1}, \tag{7}$$

where

$$\Phi_0(x) = K_1(\lambda\bar{x})Z_1^+(j-1) + \frac{K_2(\lambda\bar{x})}{\lambda} Z_2^+(j-1)$$

$$+ \frac{K_4(\lambda\bar{x})}{EI\lambda^3} Z_3^+(j-1) - \frac{K_3(\lambda\bar{x})}{EI\lambda^2} Z_4^+(j-1),$$

$$K_1(x) = \frac{\cosh x + \cos x}{2}, \quad K_2(x) = \frac{\sinh x + \sin x}{2},$$

$$K_3(x) = \frac{\cosh x - \cos x}{2}, \quad K_4(x) = \frac{\sinh x - \sin x}{2}.$$

Using the notations

$$\bar{\mathbf{R}}_j = \{r_1(\ell_j), r_2(\ell_j), r_3(\ell_j), r_4(\ell_j)\}^{\mathrm{T}}, \quad j = 1, 2, \dots, n+1,$$

where functions $r_j(x)$, $j = 1, 2, 3, 4$, have the form

$$r_1(x) = \frac{1}{\lambda^3}\int_0^x K_4(\lambda(x-\tau))\tilde{q}(x_{j-1}+\tau, \omega)\,\mathrm{d}\tau,$$

$$r_2(x) = \frac{1}{\lambda^2}\int_0^x K_3(\lambda(x-\tau))\tilde{q}(x_{j-1}+\tau, \omega)\,\mathrm{d}\tau,$$

$$r_3(x) = -EI\int_0^x K_1(\lambda(x-\tau))\tilde{q}(x_{j-1}+\tau, \omega)\,\mathrm{d}\tau,$$

$$r_4(x) = \frac{EI}{\lambda}\int_0^x K_2(\lambda(x-\tau))\tilde{q}(x_{j-1}+\tau, \omega)\,\mathrm{d}\tau, \tag{8}$$

in accordance with the transfer matrix method, one will get

$$\bar{\mathbf{Z}}^+(j) = \underline{\mathbf{Q}}(j)\bar{\mathbf{Z}}^+(j-1) + \underline{\mathbf{J}}_j\bar{\mathbf{R}}_j, \quad j = 1, 2, \ldots, n. \tag{9}$$

Here $\underline{\mathbf{Q}}(j) = \underline{\mathbf{J}}_j\underline{\mathbf{T}}_j$, where

$$\underline{\mathbf{J}}_j = [J(\alpha_j)] = \begin{bmatrix} 1 & 0 & 0 & 0 \\ 0 & 1 & 0 & \alpha_j \\ 0 & 0 & -1 & 0 \\ 0 & 0 & 0 & -1 \end{bmatrix}, \quad j = 1, 2, \ldots, n, \quad \alpha_j = \frac{6\pi(1-v^2)h}{EI} I_c\left(\frac{a_j}{h}\right)$$

and $\underline{T}_j = \underline{T}(\lambda, \ell_j)$ with the matrix function

$$\underline{\mathbf{T}}(\lambda, x) = \begin{bmatrix} K_1(\lambda x) & \lambda^{-1}K_2(\lambda x) & K_4(\lambda x)/EI\lambda^3 & -K_3(\lambda x)/EI\lambda^2 \\ \lambda K_4(\lambda x) & K_1(\lambda \ell_j) & K_3(\lambda x)/EI\lambda^2 & -K_2(\lambda x)/EI\lambda \\ -\lambda^3 EI K_2(\lambda x) & -\lambda^2 EI K_3(\lambda x) & -K_1(\lambda x) & \lambda K_4(\lambda x) \\ \lambda^2 EI K_3(\lambda x) & \lambda EI K_4(\lambda x) & \lambda^{-1}K_2(\lambda x) & -K_1(\lambda x) \end{bmatrix}.$$

Finally, applying consequently formula (9) for $j = 1, 2, \ldots, n$ leads to the equation

$$\bar{\mathbf{Z}}^-(n+1) = \mathbf{Q}\bar{\mathbf{Z}}^+(0) + \bar{\mathfrak{R}} \tag{10}$$

with the matrix $\underline{\mathbf{Q}}$ of the form

$$\underline{\mathbf{Q}} = \underline{\mathbf{T}}_{n+1}\underline{\mathbf{J}}_n\underline{\mathbf{T}}_n\,\underline{\mathbf{J}}_{n-1}, \ldots, \underline{\mathbf{J}}_2\,\underline{\mathbf{T}}_2\,\underline{\mathbf{J}}_1\,\underline{\mathbf{T}}_1 \tag{11}$$

and

$$\begin{aligned} \bar{\mathfrak{R}} &= \{\mathfrak{R}_1, \ldots, \mathfrak{R}_4\}^{\mathrm{T}} \\ &= \bar{\mathbf{R}}_{n+1} + \underline{\mathbf{T}}_{n+1}\underline{\mathbf{J}}_n\underline{\mathbf{R}}_n + \underline{\mathbf{T}}_{n+1}\underline{\mathbf{J}}_n\underline{\mathbf{T}}_n\underline{\mathbf{J}}_{n-1}\bar{\mathbf{R}}_{n-1} + \cdots + \underline{\mathbf{T}}_{n+1}\underline{\mathbf{J}}_n\underline{\mathbf{T}}_n \cdots \underline{\mathbf{J}}_2\underline{\mathbf{T}}_2\underline{\mathbf{J}}_1\bar{\mathbf{R}}_1. \end{aligned} \tag{12}$$

For convenience, the matrix $\underline{\mathbf{Q}}$ is rewritten as

$$\underline{\mathbf{Q}} = \begin{bmatrix} \underline{\mathbf{Q}}_1 & \underline{\mathbf{Q}}_2 \\ \underline{\mathbf{Q}}_3 & \underline{\mathbf{Q}}_4 \end{bmatrix},$$

where $\underline{\mathbf{Q}}_j$, $j = 1, 2, 3, 4$, are the following 2×2 matrices:

$$\underline{\mathbf{Q}}_1 = \begin{pmatrix} Q_{11} & Q_{12} \\ Q_{21} & Q_{22} \end{pmatrix}, \quad \underline{\mathbf{Q}}_2 = \begin{pmatrix} Q_{13} & Q_{14} \\ Q_{23} & Q_{24} \end{pmatrix}, \quad \underline{\mathbf{Q}}_3 = \begin{pmatrix} Q_{31} & Q_{32} \\ Q_{41} & Q_{42} \end{pmatrix}, \quad \underline{\mathbf{Q}}_4 = \begin{pmatrix} Q_{33} & Q_{34} \\ Q_{43} & Q_{44} \end{pmatrix}.$$

In the last equations, Q_{ij} are elements of the transfer matrix $\underline{\mathbf{Q}}$. Furthermore, using these notations for the vector of the nodal displacements and vector of the end forces

$$\bar{\mathbf{U}} = \{U_1, U_2, U_3, U_4\}^{\mathrm{T}}, \qquad \bar{\mathbf{P}} = \{P_1, P_2, P_3, P_4\}^{\mathrm{T}},$$

equation (10) in combination with the boundary conditions (6) is transformed into the matrix equations

$$\underline{\mathbf{K}}_U\bar{U} + \underline{\mathbf{K}}_P\bar{P} = \bar{\mathfrak{R}}, \qquad \underline{\mathbf{B}}_U\bar{U} + \underline{\mathbf{B}}_P\bar{P} = \{0\}, \tag{13}$$

where

$$\underline{\mathbf{K}}_U = \begin{bmatrix} \underline{\mathbf{Q}}_1 & -\mathrm{I} \\ \underline{\mathbf{Q}}_3 & 0 \end{bmatrix}, \quad \underline{\mathbf{K}}_P = \begin{bmatrix} \underline{\mathbf{Q}}_2 & -\mathrm{I} \\ \underline{\mathbf{Q}}_4 & 0 \end{bmatrix}, \quad \underline{\mathbf{B}}_U = \begin{bmatrix} \underline{\mathbf{B}}_1^0 & 0 \\ 0 & \underline{\mathbf{B}}_1^L \end{bmatrix}, \quad \underline{\mathbf{B}}_P = \begin{bmatrix} \underline{\mathbf{B}}_2^0 & 0 \\ 0 & \underline{\mathbf{B}}_2^L \end{bmatrix}.$$

The matrix

$$\underline{\mathbf{K}} = \begin{bmatrix} \underline{\mathbf{Q}}_1 & -\mathbf{I} & \underline{\mathbf{Q}}_2 & 0 \\ \underline{\mathbf{Q}}_3 & 0 & \underline{\mathbf{Q}}_4 & -\mathbf{I} \\ \underline{\mathbf{B}}_1^0 & 0 & \underline{\mathbf{B}}_2^0 & 0 \\ 0 & \underline{\mathbf{B}}_1^L & 0 & \underline{\mathbf{B}}_2^L \end{bmatrix} \tag{14}$$

is an (8×8) dimensional matrix here called the dynamic stiffness matrix for a multiple-cracked beam. The vector $\bar{\mathbf{F}} = \{\Re, \{0\}\}^{\mathrm{T}}$ denotes generalized load vector and $\bar{\mathbf{D}} = \{\bar{\mathbf{U}}, \bar{\mathbf{P}}\}^{\mathrm{T}}$ is generalized displacement vector. The system of equations (13), which can now be written as

$$\underline{\mathbf{K}}\bar{\mathbf{D}} = \bar{\mathbf{F}} \tag{15}$$

has to be solved in order to obtain vectors $\bar{\mathbf{Z}}^+(0)$, $\bar{\mathbf{Z}}^-(n+1)$ as solution. The vector $\bar{\mathbf{Z}}^+(0)$ would be used to determine step by step the state vectors $\bar{\mathbf{Z}}^+(j)$, $j = 1, 2, \ldots, n$ using equations (9). After that, solution of equation (4) could be found in the form of expressions (7) or the equivalent ones

$$\bar{Z}^+(j) = \underline{Q}(j)\bar{Z}^+(j-1) + \underline{J}_j\bar{R}_j, \quad j = 1, 2, \ldots, n,$$
$$\bar{Z}(x) = \underline{T}(\lambda, \bar{x})\bar{Z}^+(j-1) + \bar{R}(\bar{x}), \quad \bar{x} = x - x_{j-1} \tag{16}$$

with the functions

$$\bar{\mathbf{R}}(\bar{x}) = \{r_1(\bar{x}), r_2(\bar{x}), r_3(\bar{x}), r_4(\bar{x})\}^{\mathrm{T}},$$
$$\bar{\mathbf{Z}}(x) = \{Z_1(x), Z_2(x), Z_3(x), Z_4(x)\}^{\mathrm{T}} = \{\Phi(x), \Phi'(x), -EI\Phi'''(x), EI\,\Phi''(x)\}^{\mathrm{T}}.$$

The complex amplitude of transverse vibration for the beam thus has been obtained. The obtained equations are available for general linear boundary conditions, from which the classical cases can be obtained trivially by choosing the specific matrices $\underline{\mathbf{B}}_j$.

Thus, the dynamic stiffness matrix method applied to solve the vibration problem of a multiple-cracked beam involves the following tasks:

(1) Constructing the stiffness matrix $\underline{\mathbf{K}}$ in accordance with formulas (14), (11), (6).
(2) Calculating the load vector $\bar{\mathbf{F}}$ by using formulas (12).
(3) Solving equation (15) resulted in the state vector $\{\mathbf{Z}^+(0)\}$.
(4) Determining the state vectors $\bar{\mathbf{Z}}^+(j)$, $j = 1, 2, \ldots, n$ and afterward, the complex amplitude (or consequently, the spectrum) of displacement, slope, shear force and bending moment along the beam are calculated by using equation (16).

The problem for free vibration of the multiple-cracked beam has been investigated in reference [11]. The static and dynamic analysis problems of the beam under external load will be investigated in subsequent sections.

4. STATIC ANALYSIS FOR MULTIPLE-CRACKED BEAM (ANALYTICAL SOLUTION)

Let us consider a particular case of the vibration analysis problem, when the excitation frequency equals zero. This is the static analysis problem for the multiple-cracked beam. In this case, equation (15) becomes

$$\underline{\mathbf{K}}^0\,\bar{\mathbf{D}}^0 = \bar{\mathbf{F}}^0, \tag{17}$$

where $\underline{\mathbf{K}}^0 = \lim_{\omega\to 0}\underline{\mathbf{K}}$, $\bar{\mathbf{F}}^0 = \lim_{\omega\to 0}\bar{\mathbf{F}}$. These matrices can be calculated from equations (11) and (12). Solution of equation (17) resulted in response (displacement, slope, shear force and bending moment) to static load. For illustration, a cantilever beam subjected to a load concentrated at a point is considered. In this case, the boundary condition matrices are

$$\underline{\mathbf{B}}_2^0 = \underline{\mathbf{B}}_1^L = 0, \qquad \underline{\mathbf{B}}_1^0 = \underline{\mathbf{B}}_2^L = \mathbf{I}_2.$$

For the case of uncracked beam, i.e., $n = 0$, one has

$$\underline{\mathbf{Q}}_1 = \begin{bmatrix} 1 & L \\ 0 & 1 \end{bmatrix}, \quad \underline{\mathbf{Q}}_2 = \frac{L}{6EI}\begin{bmatrix} L^2 & -3L \\ 3L & -6 \end{bmatrix}, \quad \underline{\mathbf{Q}}_3 = \begin{bmatrix} 0 & 0 \\ 0 & 0 \end{bmatrix}, \quad \underline{\mathbf{Q}}_4 = \begin{bmatrix} -1 & 0 \\ L & -1 \end{bmatrix}.$$

If the load is concentrated at the point x_0 and has the magnitude q_0, then $\tilde{q} = -(q_0/EI)\delta(x - x_0)$ and, in consequence, the load vector can be calculated as

$$\tilde{F}_1 = -6\,\frac{q_0(L - x_0)^3}{EI}, \quad \tilde{F}_1 = -\frac{q_0(L - x_0)^2}{2EI},$$

$$\tilde{F}_3 = q_0, \quad \tilde{F}_4 = -q_0(L - x_0).$$

In this case, equation (16) yields the solution

$$U_3 = -\frac{q_0(3L - x_0)x_0^2}{6EI}, \quad U_4 = -\frac{q_0 x_0^2}{2EI},$$

$$P_1 = q_0, \quad P_2 = q_0 x_0, \; U_1 = U_2 = P_3 = P_4 = 0$$

and

$$\Phi(x) = \frac{q_0}{6EI}\left[x^3 - 3x^2 x_0 - \begin{cases} 0 & \text{if } x \leqslant x_0 \\ (x - x_0)^3 & \text{for } x \geqslant x_0 \end{cases}\right].$$

This solution is well known as an elementary solution in the theory of beam. If $x_0 = L$, the transverse displacement and slope at the free end of the beam are simplified as

$$U_3^0 = -\frac{q_0 L^3}{3EI}, \qquad U_4^0 = -\frac{q_0 L^2}{2EI}. \tag{18}$$

In the case of a single crack at x_1 with the magnitude $\beta_1 = 6\pi(1 - \nu^2)hI_c(a_1/h)$ and for the load concentrated at the free end of the beam, by analogy, one can get the solution

$$P_1 = q_0, \quad P_2 = q_0 L, \quad U_3 = -\frac{q_0 L^3}{3EI}\left(1 + \frac{3\beta_1(L - x_1)^2}{L^3}\right), \quad U_4 = -\frac{q_0 L^2}{2EI}\left(1 + \frac{2\beta_1(L - x_1)}{L^2}\right).$$

Comparing U_3, U_4 in the above formulas obtained for cracked beam with the one given by formulas (18) for the uncracked beam, the amplification factors of displacement and slope due to crack can be obtained as

$$A_3 \cong \frac{U_3}{U_3^0} = 1 + \frac{3\beta_1(L - x_1)^2}{L^3}, \qquad A_4 \cong \frac{U_4}{U_4^0} = 1 + \frac{2\beta_1(L - x_1)}{L^2}. \tag{19}$$

From formulas (19), it can be seen that the amplification factors reach their maximum for a crack that appears close to the fixed end and minimum (equal to 1) for a crack close to the free end of the beam. Of course, the factors increase as the crack depth increases. If the crack depth equals zero these factors get unique value, i.e., no crack has occurred. In such a way, one can study the effect of two, three or more cracks on the static behaviour of beam with different boundary conditions. In fact, the amplification factors for static displacements of a cantilever beam in the case of n cracks at $x_1, \ldots, x_n$ with magnitudes $\beta_1, \ldots, \beta_n$ can be calculated (at the free end under the load applied at the point) as

$$A_3 = 1 + \sum_{j=1}^{n} \frac{3\beta_j (L - x_j)^2}{L^3}, \qquad A_4 = 1 + \sum_{j=1}^{n} \frac{2\beta_j (L - x_j)}{L^2}. \tag{19'}$$

In general, static response of a multiple-cracked beam can be conducted from the dynamic one (solution of equation (15)) by substituting into it zero frequency. This will be seen in the next section, where the dynamic response of a cantilever with a number of cracks is investigated numerically.

5. FORCED VIBRATION OF A MULTIPLE-CRACKED CANTILEVER BEAM (NUMERICAL RESULTS)

To illustrate the above-developed method for multiple-cracked beam, a numerical investigation is carried out in this section for the cantilever that was considered in reference [13]. The steel beam has rectangular section $0{\cdot}2\,\text{m} \times 0{\cdot}2\,\text{m}$ and length 3 m. A harmonic exciting force of the amplitude $P_0 = 3000\,\text{N}$ and frequency ω is applied at the point 1 m from the free end of the beam. Open transverse cracks of depth a_i, $i = 1, 2, \ldots$, have been assumed to appear at the locations starting from the point 1 m from the left end of the beam and continue to the right with a distance of 0·07 m between each other. Young's modulus $E = 2{\cdot}1 \times 10^{11}\,\text{N/m}^2$, material density $\rho = 7850\,\text{kg/m}^3$ and damping coefficients $\mu_1 = 0{\cdot}002$, $\mu_2 = 0$.

Firstly, the case of single crack at $x_1 = 1$ m with depths of 0; 4; 8 and 12 mm is studied and results are given in Figures 2–7. In Figures 2–4, the dynamic transverse displacement, slope, bending moment and shear force distributed along the beam are shown. In each figure four curves correspond to different depths of crack, equal to 0, 20, 40, 60% of the beam height. These results were computed at the exciting frequency of 60 rad/s. Obviously, the increase of crack depth leads to growth of vibration amplitude and this effect will be more significant at

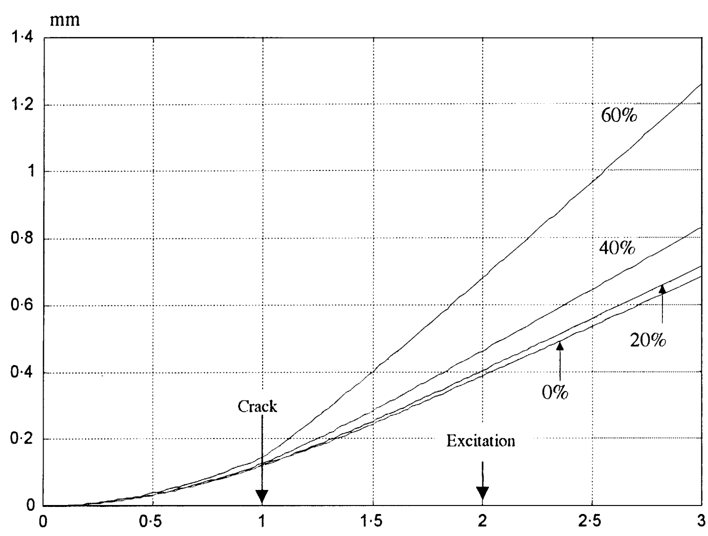

Figure 2. Vibration amplitude along the beam in the case of single crack with different depths, exciting frequency 60 rad/s.

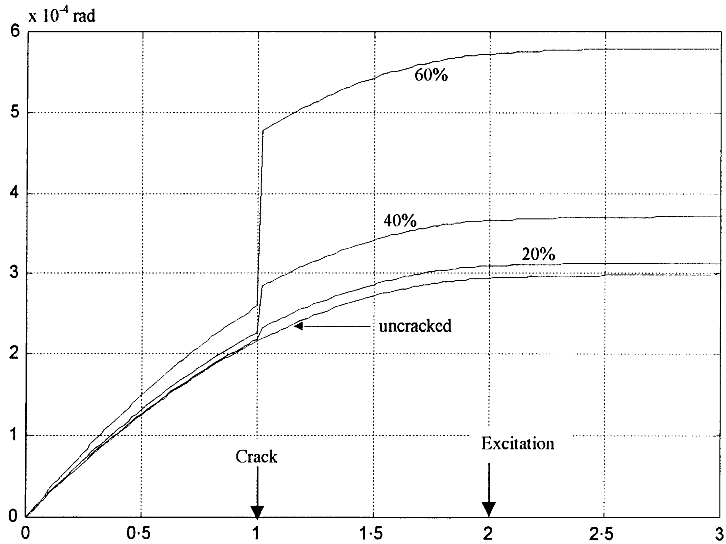

Figure 3. Slope along the beam with single crack of different depths, exciting frequency 60 rad/s.

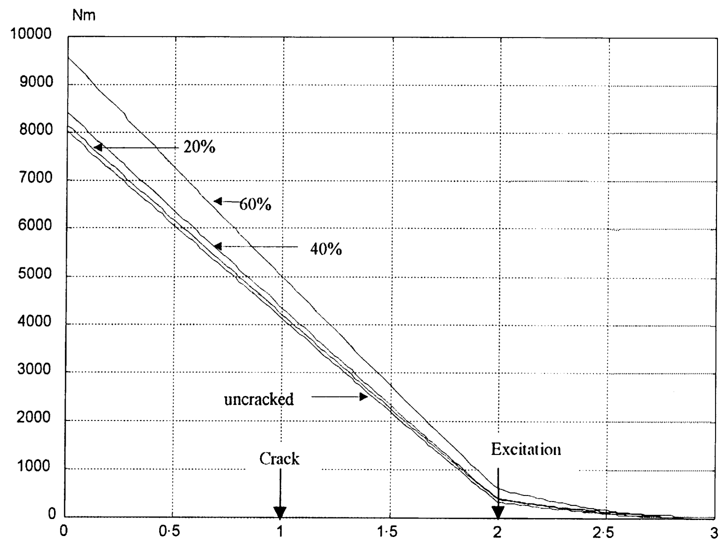

Figure 4. The bending moment along the beam for different crack depths, at frequency 60 rad/s.

greater depth. Furthermore, the slope gets a jump at the crack position, but shear force has a jump at the point where the excitation is applied. The spectrum of displacement and slope of the free end of beam are presented in Figures 6 and 7, which show clearly the first resonant peaks corresponding to different crack depths. Here, it is seen that crack reduces the resonant frequencies of beam and crack depth growth increases the resonant vibration amplitude. In this case of loss coefficient of beam material, the second resonant peaks do not appear in the spectrum. Analogously, frequency response can be computed at the point of excitation (2 m). Results of computation show that vibration amplitude at point of

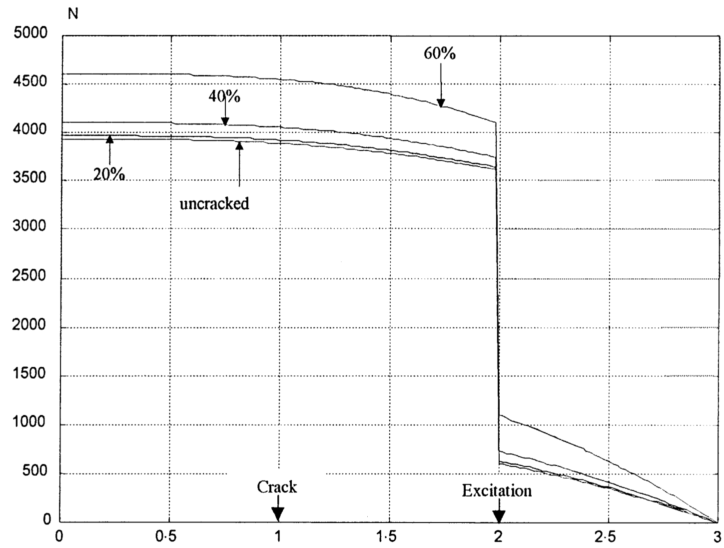

Figure 5. The shear force along the beam for different crack depths, at frequency 60 rad/s.

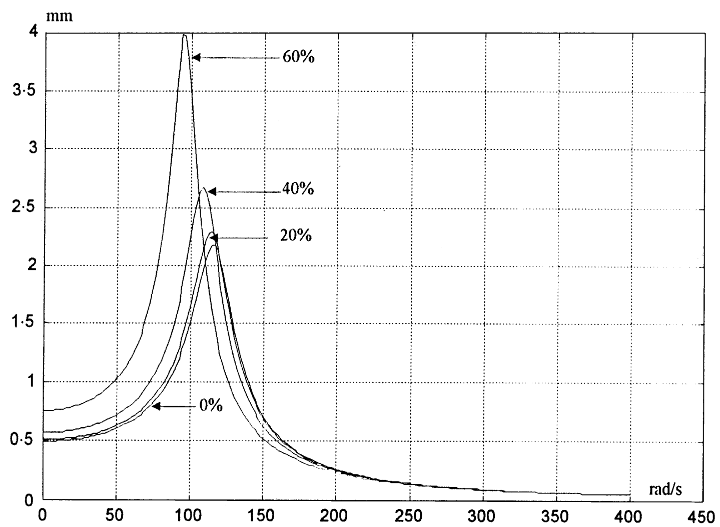

Figure 6. Displacement spectrum of the free end in the case of a single crack with different depths ($a/h = 0$; 0·2; 0·4; 0·6).

excitation compared to that obtained at the free end (Figure 6) is reduced approximately to a half and the slope has not been changed significantly.

Furthermore, the influence of quantity of cracks on forced vibration of the cantilever is investigated numerically. Figures 8–11 show the vibration amplitude and slope with respect to exciting frequency (spectrum) and along the beam with various numbers of cracks (from 1 to 10 cracks). It is similar to the crack depth, the number of cracks increases the amplitude of vibration and reduces the resonant frequencies of the beam. However, the vibration amplitude and resonant frequencies are more sensitive to the number of cracks at its

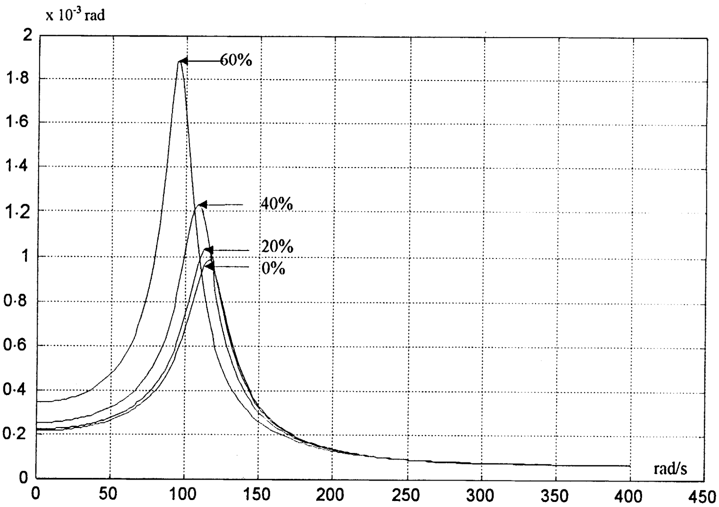

Figure 7. Slope spectrum at the free end of beam with a single crack of different depths ($a/h = 0$; 0·2; 0·4; 0·6).

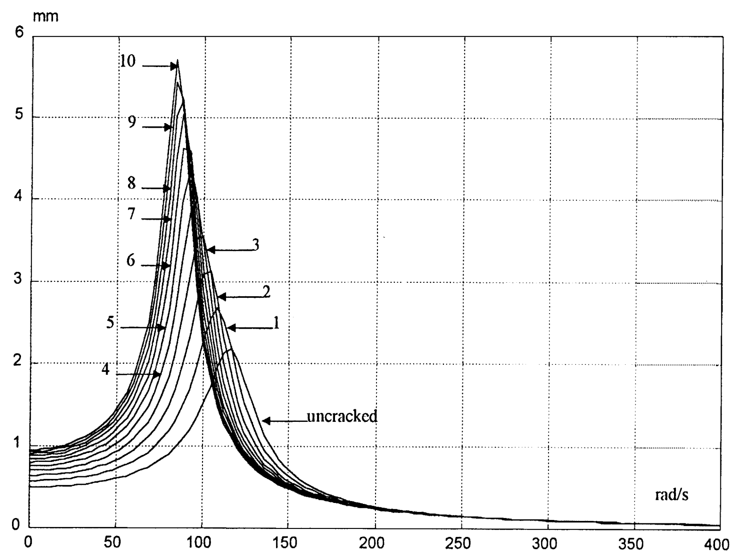

Figure 8. Vibration amplitude spectrum at the free end of beam for different numbers of cracks.

lower value. This effect may imply that the presence of a crack and its depth play a more important role than the number of cracks. Figure 11 also shows the discontinuity of slope at the crack locations. The effect of the loss coefficient μ_1 on the spectrum of displacement and slope is shown in Figures 12 and 13. These graphics have been obtained in the case of a single crack at position 1 m with a depth of 60% of beam height. It is interesting to note that the loss coefficient compared to the crack depth results in greater effect.

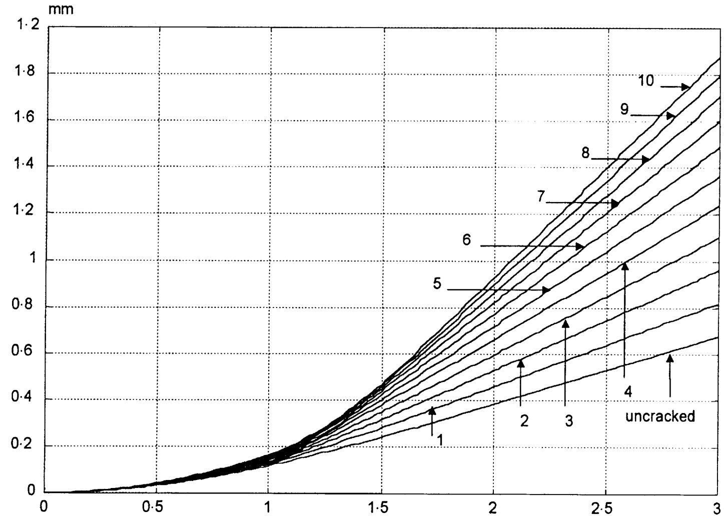

Figure 9. Vibration amplitude along the beam for different numbers of cracks, exciting frequency 60 rad/s.

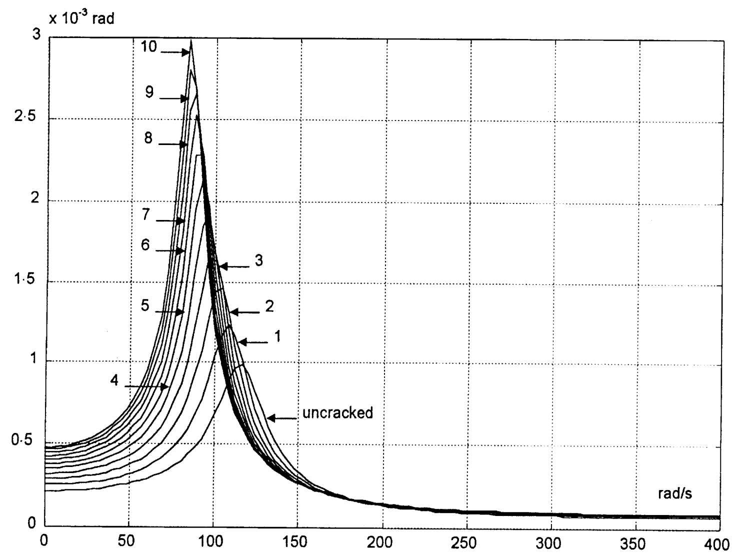

Figure 10. Slope spectrum at the free end of beam for different numbers of cracks.

6. COMPARISON AND DISCUSSION

Forced vibration of a beam with single transverse crack has been studied in references [12, 13]. Authors of the work [13] have constructed the finite element matrices of mass and stiffness for a cracked beam based on the concept of a crack compliance matrix and the finite element procedure. In fact, the crack compliance introduced in the paper related to a discontinuity in the deflection and slope due to the presence of crack. However, as shown

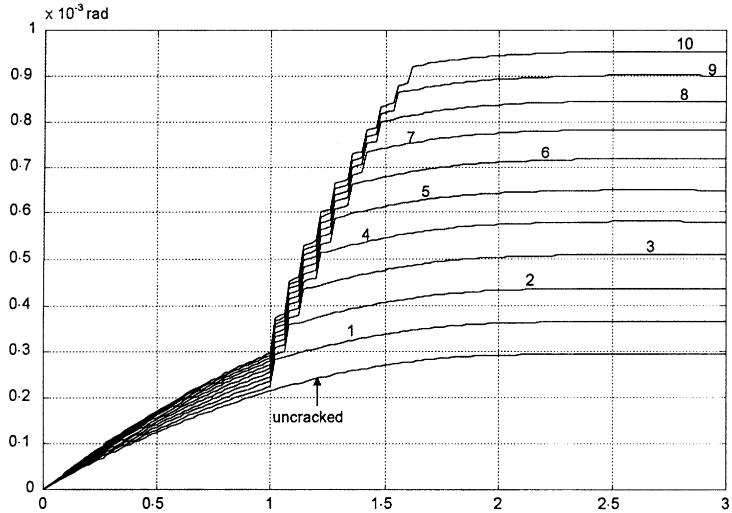

Figure 11. Slope along the beam with different numbers of cracks, exciting frequency 60 rad/s.

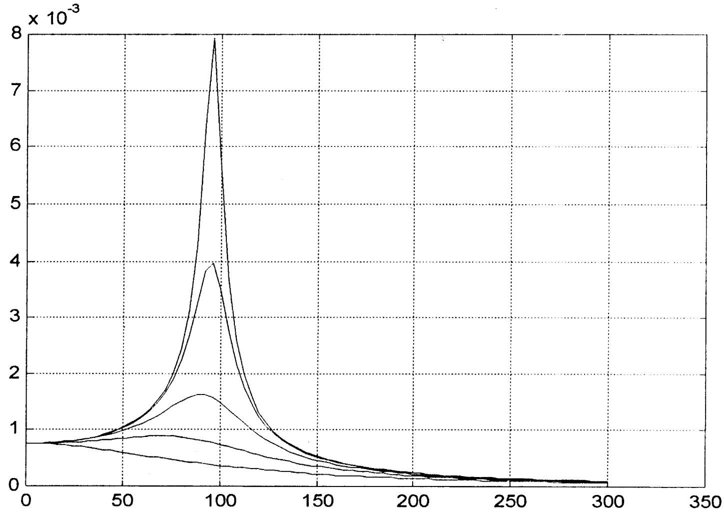

Figure 12. The displacement spectrum for different values of damping coefficient $\mu_1 = 0{\cdot}001$; 0·002; 0·005; 0·01; 0·02.

in Figures 4 and 5 of the paper, only a jump in slope is presented. Thus, the model of crack proposed above in this paper is valid. For comparison, relative vibration amplitude along the beam at frequency 60 rad/s has been computed and shown in Figure 14. A comparison of the result and that given in Figure 4 of reference [13] shows the good agreement of the two approaches. On the other hand, the loss coefficient γ introduced and then chosen to equal 0·002 by the authors of reference [13] is not correct. The loss coefficient must depend on the frequency and must be multiplied by the frequency ω in the equation of motion. Such a chosen loss coefficient is so small that the second resonant peaks in the spectrum graphic

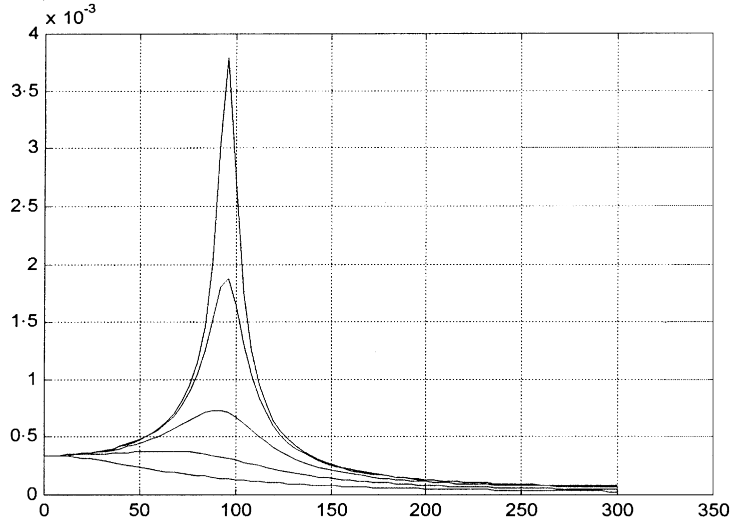

Figure 13. Slope spectrum for different values of damping coefficient $\mu_1 = 0{\cdot}001$; $0{\cdot}002$; $0{\cdot}005$; $0{\cdot}01$; $0{\cdot}02$.

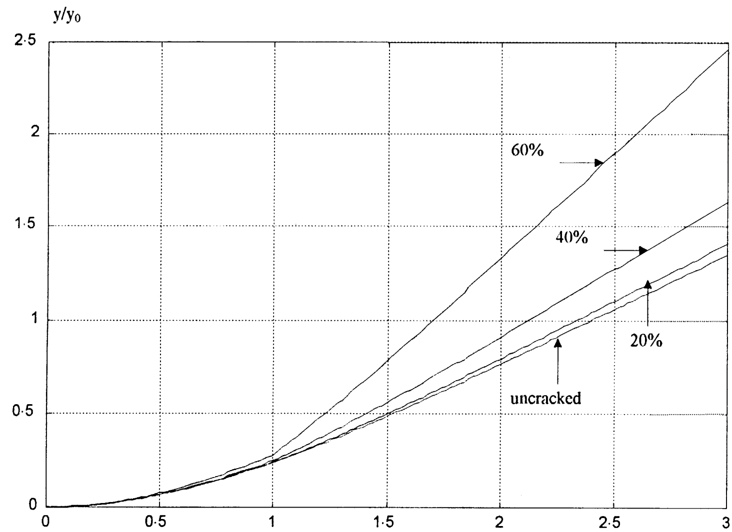

Figure 14. Relative vibration amplitude along the beam with a single crack of different depths, excitation frequency 60 rad/s.

of vibration amplitude have not been presented (Figure 3 in reference [13]). Furthermore, it is difficult to explain the fact that according to the above-mentioned figure crack depth does not affect the vibration amplitude at the first resonant frequency and it even reduces the amplitude of second resonant vibration when the relative crack depth $a/h = 0{\cdot}6$. This unlikelihood may be caused by the incorrect loss coefficient used.

The numerical results obtained in the previous section have been checked also by comparison with the well-known static response of a cantilever to a concentrated load.

The dynamic stiffness matrix method considered herein is one of the exact methods for multiple-cracked beam and it is a basis to develop the method for analysis of frame structures. The equations and analytical solutions obtained in this work are useful in the crack detection problem of structures.

ACKNOWLEDGMENTS

This work has been completed with moral and financial support from the National Council in Natural Sciences of Vietnam, to whom the authors are greatly thankful.

REFERENCES

1. H. SATO 1983 *Journal of Sound and Vibration* **89**, 59–64. Free vibration of beams with abrupt changes of cross-section.
2. P. GUDMUNSON 1983 *Journal of Mechanics and Physics of Solids* **31**, 329–345. The dynamic behaviour of slender structures with cross-sectional cracks.
3. M. M. F. YUEN 1985 *Journal of Sound and Vibration* **103**, 301–310. A numerical study of the eigenparameters of a damaged cantilever.
4. M.-H. H. SHEN and C. PIERRE 1990 *Journal of Sound and vibration* **138**, 115–134. Natural modes of Bernoulli–Euler beam with symmetric cracks.
5. T. G. CHONDROS, A. D. DIMAROGONAS and J. YAO 1998 *Journal of Sound and Vibration* **215**, 17–34. A continuous cracked beam vibration theory.
6. R. Y. LIANG, J. HU and F. CHOY 1992 *Journal of Engineering Mechanics* **118**, 384–396. Theoretical study of crack-induced eigenfrequency change on beam structures.
7. A. MORSASI 1992 *Journal of Engineering Mechanics* **119**, 1798–1803. Crack-induced changes in eigenparameters of beam structures.
8. M. CHARTI, R. RAND and S. MUKHERJEE 1997 *Journal of Sound and Vibration* **207**, 249–270. Modal analysis of cracked beam.
9. E. I. SHIFRIN and R. RUOTOLO 1999 *Journal of Sound and Vibration* **222**, 409–423. Natural frequencies of a beam with an arbitrary number of cracks.
10. A. S. SEKHAR 1999 *Journal of Sound and Vibration* **223**, 497–512. Vibration characteristics of a cracked rotor with two open cracks.
11. N. T. KHIEM and T. V. LIEN 2001 *Journal of Sound and Vibration* **245**, 737–751. A simplified method for frequency analysis of multiple cracked beam.
12. W. M. OSTACHOWICZ and M. KRAWCZUK 1990 *Computers & Structures* **36**, 245–250. Vibration analysis of cracked beam.
13. G. GOUNARIS and A. DIMAROGONAS 1988 *Computers & Structures* **28**, 309–313. A finite element of a cracked prismatic beam for structural analysis.
14. B. S. HAISTY and W. T. SPRINGER 1988 *Transactions of the American Society of Mechanical Engineers, Journal of Vibration Acoustics, and Stress Reliability Design* **110**, 389–394. A general beam element for use in damage assessment of complex structures.
15. N. C. MENH, N. T. KHIEM, D. N. MAI and N. V. KHOA 1998 *Vietnam Journal of Mechanics* N. I. T. **XX**, 29–46. Modal analysis of damaged structures by the modified finite element method.
16. T. H. RICHARDS and Y. T. LEUNG 1977 *Journal of Sound and Vibration* **55**, 363–376. An accurate method in structural vibration analysis.
17. A. Y. T. LEUNG 1993 *Dynamic Stiffness and Substructures*, 242. London: Springer-Verlag.
18. A. Y. T. LEUNG 2001 *Journal of Sound and Vibration* **242**, 377–395. Dynamic stiffness for structures with distributed deterministic or random loads.